JOURNAL OF SOLID STATE CHEMISTRY 103, 193–207 (1993)

Cation Distribution and Local Configuration of Fe^{2+} Ions in Structurally Nonequivalent Lattice Sites of Heterometallic Fe(II)/*M*(II) (*M* = Mn, Co, Ni, Cu, Zn) Diaquadiformato Complexes

M. DEVILLERS* AND J. LADRIÈRE

Université Catholique de Louvain, Laboratoire de Chimie Inorganique et Nucléaire, Chemin du Cyclotron, 2, B-1348 Louvain-la-Neuve, Belgium

Received April 27, 1992; accepted August 21, 1992

^{57}Fe Mössbauer investigations are carried out on a wide series of heterometallic diaquadiformato Fe(II)/*M*(II) complexes with *M* = Mn, Co, Ni, Cu, and Zn to provide a local picture of the coordination environment of the $^{57}Fe^{2+}$ ions as a function of (i) the nature of the host cation and (ii) the relative amounts of both metals in the matrix (between 50 and 0.25 at.% Fe). Information is obtained on the quantitative distribution of both metals between the two structurally nonequivalent lattice sites and on the local geometry around the dopant atom in each crystal site. In the mixed Fe–Cu complexes, Fe^{2+} ions are preferentially incorporated in the tetrahydrated site; in Cu-rich $Fe_xCu_{1-x}(HCO_2)_2 \cdot 2H_2O$, the $^{57}Fe^{2+}$ ions located in the hexaformato-coordinated site are surrounded by an axially compressed octahedron of formate ligands which contrasts with the elongated configuration observed in the pure iron compound and in the other mixed systems. Semiquantitative estimations of the tetragonal field splitting and of the extent of metal–ligand interactions are proposed from the temperature dependence of the quadrupole splitting values.

Introduction

In several solid-state spectroscopic techniques such as EPR and Mössbauer spectroscopy, dopant atoms are commonly used as internal probes for the *in situ* structural, electronic, and/or magnetic characterization of host matrices. Even within an isostructural series which furthers substitutional replacement of the host cation by the dopant ion, the question of whether the probe nucleus faithfully reflects the local configuration of the host cation site under consideration remains of interest. In the frame of emission Mössbauer spectroscopy studies on the physicochemical consequences of nuclear decays in some carboxylates, we described some time ago local covalency and lattice effects in the isostructural series of mixed oxalate complexes having the general formula $Fe_xM_{1-x}C_2O_4 \cdot 2H_2O$ with *M* = Mg, Mn, Co, Ni, and Zn (*1*). Accurate knowledge of the local symmetry around the ^{57}Fe Mössbauer probe in these compounds was actually essential to provide unequivocal and coherent interpretations of the influence of the host cation nature on the chemical aftereffects associated with the electron capture decay of ^{57}Co into ^{57}Fe in the corresponding ^{57}Co-doped compounds (*2*).

An additional center of interest concerns systems containing two or more structurally nonequivalent lattice sites, for which cat-

* Chercheur qualifié F.N.R.S.

0022-4596/93 $5.00

ions of different natures may display some preference for occupying one of the available sites in the mixed crystals. The present work deals with a ^{57}Fe Mössbauer study of the heterometallic diaquadiformato Fe(II)–M(II) complexes ($Fe_xM_{1-x}(HCO_2)_2 \cdot 2H_2O$) with M = Mn, Co, Ni, Cu, and Zn. In these compounds, the metal cations are known to occupy two distinct lattice sites corresponding to the compositions $[M(HCO_2)_6]^{4-}$ and $[M(H_2O)_4(HCO_2)_2]$, displaying O_h- and D_{4h}-type symmetry, respectively. Because the Cu^{2+} ions give rise to marked tetragonal Jahn–Teller distortions, special interest has been devoted in the past to the mixed M(II)–Cu(II) formates. Crystallographic data and infrared measurements indicated a nonuniform distribution of the two cations between the two lattice sites in the Cu–Zn (*3*, *4*), Cu–Mg (*5*), and Cu–Cd (*6*) systems. In the first two cases, the Cu^{2+} ions were found to exhibit a clear preference for the hexaformato-coordinated site; more recent diffuse reflectance spectroscopy experiments in the visible range on $Cd_{1-x}Cu_x(HCO_2)_2 \cdot 2H_2O$ mixed crystals, however, provided evidence for the exclusive incorporation of Cu^{2+} ions at $x < 0.5$ in the mixed coordination environment. Furthermore, the pronounced Jahn–Teller effect was suggested to be responsible for the interruption in the Cu(II)–Co(II) mixed crystals series, resulting in a phase transition in the Cu-rich region (*7*).

In order to widen these studies to iron-containing mixed crystals, the Mössbauer technique is now used in the absorption mode to characterize the local coordination environment of Fe^{2+} ions in the isostructural series $M_{1-x}Fe_x(HCO_2)_2 \cdot 2H_2O$ as a function of (i) the nature of the host cation M, and (ii) the relative amounts of both metals in the matrix (between 50 and 0.25 at.% Fe). As far as the Lamb–Mössbauer factors of the ^{57}Fe species are assumed to be similar for the two concerned sites, information is gained on the quantitative distribution of iron among the two structurally nonequivalent lattice positions and on the local geometry around the $^{57}Fe^{2+}$ ions in each crystal site.

Experimental

The diaquadiformato compounds $M(HCO_2)_2 \cdot 2H_2O$ (with M = Mn, Co, Ni, Cu, and Zn) were obtained by neutralization of the corresponding binary carbonate with an aqueous solution of formic acid (33%) in excess. Precipitation occurred slowly at room temperature under continuous stirring upon addition of ethanol to the starting solution. The pure Fe(II) compound was obtained similarly from aqueous ferrous sulfate and sodium formate. The heterometallic Fe(II)/M(II) compounds were obtained in air-free conditions from an aqueous solution of the corresponding pure formates in the presence of some formic acid. Samples containing 5% Fe or less were synthesized using isotopically enriched ^{57}Fe.

The solids were characterized by their X-ray powder diffraction patterns obtained on a Seifert diffractometer equipped with proportional counter, using the Co$K\alpha$ radiation. The hydration content of the compounds was checked by thermogravimetric analysis under inert atmosphere using a DuPont 950 thermal analyzer.

^{57}Fe Mössbauer spectra were registered in the absorption mode at room temperature and at 80 K using a constant acceleration transducer coupled with a 512 multichannel analyzer (Northern NS-900) and a $^{57}Co/Rh$ source kept at RT. All the isomer shift values (δ) given hereafter are expressed with respect to metallic α-Fe at RT. Experimental data were resolved into Lorentzian lines using an iterative least-squares fit program.

Literature Overview of Relevant Structural and Magnetic Data

According to numerous literature data, the pure diaquadiformato compounds of

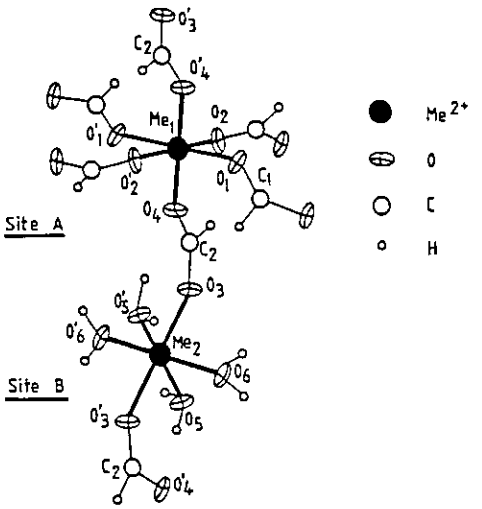

FIG. 1. Crystal structure of diaquadiformato compounds $M^{II}(HCO_2)_2 \cdot 2H_2O$ with M = Mn, Fe, Co, Ni, Cu, Zn (from Ref. (*8*)).

Fe(II) (*8*), Mn(II) (*9*), Co(II) (*10*), Ni(II) (*11*), Cu(II) (*9*, *12*), Zn(II) (*13*), Mg(II) (*14*), and Cd(II) (*15*) are isostructural and exhibit a monoclinic structure with C_{2h}^5 symmetry (Space group $P2_{1/c}$). As shown in Fig. 1, the metal cations are located in two structurally nonequivalent crystal lattice sites, both having a distorted octahedral geometry. In the A-site, the metal is octahedrally surrounded by six oxygen atoms belonging to six different formate groups which are in bridging position between adjacent metal atoms lying in the same plane. In the B-site, the six coordinating oxygen atoms belong to four water molecules and two formate ligands in *trans* position with respect to the plane containing the water molecules. In the latter site, each formate group acts as a bridging ligand between A-type and B-type metal cations. Additional hydrogen bonds between the water molecules and the oxygen atoms of the formate groups give the whole assembly a tridimensional polymeric structure consisting in alternate packing of parallel A- and B-type sheets along the ⟨100⟩ direction. Table I summarizes the main crystallographic data relevant to the subsequent discussion.

The presence of two nonequivalent coordination sites for the metal ions in these compounds gives rise to peculiar magnetic behavior at low temperature, which has been studied intensively by several techniques including NMR, neutron diffraction, magnetocalorimetry and magnetic susceptibility measurements (*16–19*). Neglecting some minor variations in their respective magnetic behavior, the Mn(II), Fe(II), Ni(II), and Cu(II) diaquadiformato compounds were shown to offer three main characteristics:

(1) upon the temperature being lowered A-type ions become magnetically ordered at a higher temperature than B-type ions, i.e., the Néel transition temperatures are in the sequence $(T_N)_A > (T_N)_B$;

(2) whereas the AA coupling is antiferromagnetic, the AB coupling is ferromagnetic and of lower intensity;

(3) the interactions between the magnetic moments of neighboring M^{2+} ions are described in terms of superexchange interactions proceeding through an excited electronic state of the formate ligand (*20*).

Results and Discussion

Diaquadiformato Iron(II)

Table II gives the Mössbauer parameters of $Fe(HCO_2)_2 \cdot 2H_2O$ obtained in this work together with previously published literature values (*21–23*). The corresponding absorption spectra are shown in Fig. 2.

In a previous work on the temperature dependence of the Fe^{2+} quadrupole splitting values in both sites (*21*), Hoy and de Barros assigned the internal doublet to the crystal site A, where the metal cation is coordinated by six identical formate groups responsible for a higher symmetry. This assignment is in agreement with the structural features observed by X-ray diffraction (*8*).

TABLE I

STRUCTURAL CHARACTERISTICS OF DIHYDRATED FORMATES OF SOME BIVALENT METALS OF THE FIRST TRANSITION SERIES

M	Mn	Fe	Co	Ni	Cu	Zn
a(Å)	8.86	8.740	8.63	8.60	8.54	8.685
b(Å)	7.18	7.192	7.06	7.06	7.15	7.160
c(Å)	9.39	9.428	9.21	9.21	9.50	9.324
β(°)	97.6	97.47	96	96.8	96.8	97.97
V(Å^3)	592.1	587.6	558.1	555.1	574.2	574.6
			Site A			
d(Å) Me_1–O_1	2.172	2.127	2.03	2.061	2.304	2.102
d(Å) Me_1–O_2	2.135	2.093	2.04	2.026	1.988	2.071
d(Å) Me_1–O_4	2.218	2.167	2.10	2.097	2.019	2.145
θ(°) O_1–Me_1–O_1	89.7	90.4	88	90.3	89.2	89.5
θ(°) O_1–Me_1–O_4	88.4	92.6	94	86.7	88.5	87.2
θ(°) O_2–Me_1–O_1	88.1	92.4	86	92.8	86.8	87.2
			Site B			
d(Å) Me_2–O_3	2.219	2.180	2.06	2.090	2.368	2.166
d(Å) Me_2–O_5(H_2O)	2.216	2.153	2.06	2.059	2.044	2.103
d(Å) Me_2–O_6(H_2O)	2.168	2.084	2.07	2.042	1.974	2.054
θ(°) O_3–Me_2–O_5	86.6	91.5	89	89.2	87.6	88.8
θ(°) O_3–Me_2–O_6	89.1	88.6	88	89.7	86.9	90.0
θ(°) O_5–Me_2–O_6	89.8	89.8	90	89.8	87.5	90.6
Ref.	(9)	(8)	(10)	(11)	(9, 12)	(13)

As obvious from the interatomic distances listed in Table I, the coordination symmetry around the Fe^{2+} ion in site A can be approximated by a tetragonally distorted octahedron with an elongation along the Fe_1–O_4 axis, i.e., perpendicular to the plane of the A-type sheets containing all the hexaformatocoordinated sites. The geometrical configuration of Fe^{2+} in site B corresponds to a slightly compressed octahedron, where the shortest iron–oxygen distance (Fe_2–O_6) is located within the plane of B-type sheets. In line with the general expression of the quadrupole splitting (Δ) of Fe^{2+} in a tetragonally distorted octahedral geometry (see Appendix), the observation of Δ-values much larger than 2 mm s^{-1} at 80 K as well as at RT allows us to assign this spectral component to the compressed site, for which theoretical limits of Δ close to 4 mm s^{-1} can be expected. Using the experimental Δ values obtained in the present work and according to considerations developed in the appendix, the tetragonal field splitting parameter Δ_3, which characterizes the energy separation between the two t_{2g}-sublevels, can be estimated for the two crystal sites as 160 cm^{-1} for site A and 645 cm^{-1} for site B. These values agree reasonably well with those ones mentioned by Hoy and de Barros, i.e., 173 and 590 cm^{-1}, respectively.

Similar conclusions can be drawn from considerations on the relative covalency effects associated with the respective H_2O and HCO_2^- ligands. These effects can be evaluated in two different ways: (1) from accurate measurement of the isomer shift values, and (2) from estimations of the so-called covalency parameter, α^2, as defined in the appendix (Eq. (5)).

TABLE II

ABSORPTION MÖSSBAUER PARAMETERS OF ^{57}Fe IN $Fe(HCO_2)_2 \cdot 2H_2O$

T (K)	Site	Δ (mm/s)[a]	δ^{Fe} (mm/s)[b]	Γ (mm/s)[c]	Ref.
80	B	3.44	1.38	0.35	
	A	1.32	1.33	0.35	(*21*)
295	B	2.96	1.25	0.27	
	A	0.65	1.21	0.29	
80	B	3.42	1.41	—	
	A	1.37	1.41	—	(*22*)
295	B	2.96	1.24	—	
	A	0.65	1.19	—	
295	B	3.02	1.23	—	
	A	0.63	1.21	—	(*23*)
80	B	3.40	1.38	0.28	[d]
	A	1.35	1.34	0.29	
295	B	2.97	1.25	0.27	
	A	0.64	1.22	0.27	

[a] Quadrupole splitting.
[b] Isomer shift relative to α-Fe.
[c] Full width at half maximum.
[d] This work. See Table III for standard errors.

The first method is based on the slight but systematic difference in δ-values for the two sites, as shown in Table II:

$$\delta_{ext} - \delta_{int} = (0.04 \pm 0.01) \text{ mm sec}^{-1},$$

where δ_{ext} and δ_{int} correspond to the external and internal components, respectively. Considering the inverse proportionality relationship between the ^{57}Fe isomer shift value and the electronic density at the ^{57}Fe nucleus, the smaller δ-value observed for the internal doublet reflects a higher electron density, i.e., a larger covalent contribution from the surrounding ligands.

A similar conclusion can be derived from the empirical covalency parameter, α^2, as defined in Eq. (5). This parameter can be estimated from the ratio of the Δ-values at 80 K and 295 K (see Eq. (10)), assuming that the lattice contribution to the electric field gradient, q_{latt}, is negligible for small geometrical distortions. On the basis of the present Δ-values (Table II), α^2-values of 0.85 and 0.75 are obtained for the external and internal component, respectively, indicating once again that a higher covalency extent is associated with the external doublet.

When translating these covalency effects in terms of σ-donor properties of the oxygen atoms, the above-described observations suggest that the internal doublet corresponds to the iron(II) site in which the oxygen-bound ligands exhibit the larger electrodonating capabilities. Whether this is a fact for H_2O or HCO_2^- can be deduced from independent experimental data, such as the ligand nephelauxetic parameter, h. Correlations between the saturation values of the internal magnetic field, H_0, of Fe^{3+}

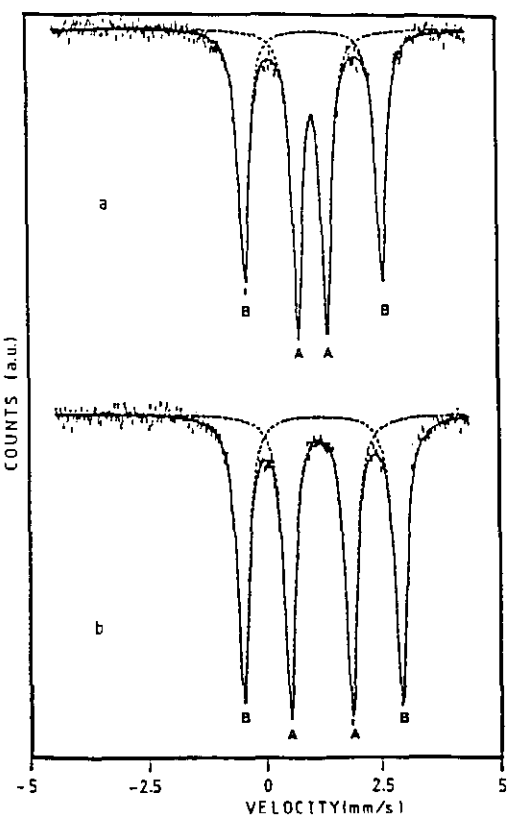

FIG. 2. ^{57}Fe absorption Mössbauer spectra of $Fe(HCO_2)_2 \cdot 2H_2O$ at (a) 295 K and (b) 80 K.

ions and the nephelauxetic parameter of the corresponding ligands indicate that the formate group has slightly larger σ-donating capabilities than water molecules (*24*). This results once more in assigning the internal doublet to the hexaformatocoordinated A site. If one admits an empirical additivity relationship of the partial nephelauxetic parameters h_i of the different coordinating ligands, and takes $h_{H_2O} = 1.00$ and $h_{HCO_2^-} = 1.20$, the following overall nephelauxetic parameters are obtained for the two sites: $h_A = 1.20$ and $h_B = 1.07$. Some indication that these data are internally consistent can be provided by comparing the ratio $h_A/h_B = 1.12$ with the reciprocal ratio of the associated covalency parameters, $\alpha_A^2/\alpha_B^2 = 1/1.13$.

Heterometallic Fe(II)/M(II) Diaquadiformato Complexes

Mössbauer parameters. Table III lists the Mössbauer parameters of ^{57}Fe in the heterometallic Fe(II)/*M*(II) dihydrated formates containing between 50 and 0.25 at.% Fe. Selected examples of experimental spectra are shown in Figs. 3a (*M* = Mn, Co, Ni) and 3b (*M* = Cu).

Cation distribution. Interpretation of the relative surfaces of Mössbauer resonance lines in terms of ratio of the corresponding species requires that identical Mössbauer–Lamb factors be assumed for the ^{57}Fe atoms in the two concerned lattice sites. These factors are related to the Debye temperature of the solid and reflect the strength of the metal–ligand bonds. Because the intensity ratio of the quadrupole doublets corresponding to the two coordination sites is close to 1.0 in the pure iron compound, the force constants of the Fe–O bonds are concluded to be similar for both the formate and the water ligands. A greater caution should be exercised in the case of the mixed Fe/*M* system: formate groups in a bridging position between cations of different nature might transfer local variations of the

TABLE III

ABSORPTION MÖSSBAUER PARAMETERS OF ^{57}Fe IN HETEROMETALLIC Fe(II)–*M*(II) DIHYDRATED FORMATES (*M* = Mn, Co, Ni, Cu, Zn)

M	%Fe[a]	*T* (K)	Site	Δ (mm/s)[b]	δ^{Fe} (mm/s)[c]	Γ (mm/s)[d]	I_B/I_A[e]
Co	50	80	B	3.38	1.37	0.31	1.00
			A	1.30	1.33	0.38	
		295	B	2.97	1.25	0.25	0.89
			A	0.68	1.22	0.29	
	10	80	B	3.33	1.36	0.28	1.27
			A	1.28	1.32	0.33	
		295	B	2.94	1.25	0.28	1.08
			A	0.67	1.22	0.32	
	5*	80	B	3.36	1.37	0.41	0.85
			A	1.31	1.33	0.44	
		295	B	2.92	1.24	0.33	0.75
			A	0.65	1.21	0.35	
	1*	80	B	3.33	1.36	0.32	0.90
			A	1.30	1.32	0.37	
		295	B	2.93	1.25	0.34	0.75
			A	0.66	1.22	0.36	
	0.25*	80	B	3.36	1.37	0.29	0.91
			A	1.33	1.32	0.37	
		295	B	2.95	1.25	0.27	0.73
			A	0.66	1.23	0.30	
Mn	50	80	B	3.42	1.37	0.29	0.89
			A	1.27	1.33	0.32	
		295	B	2.98	1.24	0.24	0.82
			A	0.61	1.22	0.25	
	5*	80	B	3.46	1.37	0.30	0.92
			A	1.17	1.34	0.31	
		295	B	3.02	1.25	0.27	0.96
			A	0.58	1.23	0.28	
	1*	80	B	3.45	1.37	0.27	0.96
			A	1.18	1.34	0.28	
		295	B	3.03	1.25	0.28	0.86
			A	0.58	1.23	0.29	
	0.25*	80	B	3.40	1.37	0.31	1.08
			A	1.16	1.34	0.30	
		295	B	3.01	1.25	0.23	0.82
			A	0.58	1.24	0.25	
Ni	50	80	B	3.35	1.36	0.29	0.89
			A	1.30	1.32	0.41	
		295	B	2.94	1.25	0.28	0.82
			A	0.70	1.22	0.32	
	1*	80	B	3.28	1.36	0.30	0.80
			A	1.26	1.27	0.38	
		295	B	2.89	1.24	0.26	0.67
			A	0.66	1.22	0.26	
Zn	50	80	B	3.38	1.37	0.29	0.92
			A	1.31	1.33	0.31	
		295	B	2.97	1.24	0.24	0.85
			A	0.64	1.21	0.26	
	0.5*	80	B	3.33	1.36	0.28	1.50
			A	1.11	1.30	0.31	
		295	B	2.95	1.26	0.32	1.32
			A	0.67	1.20	0.33	
Cu	50	80	B	3.35	1.36	0.30	1.09
			A	1.51	1.33	0.55	
		295	B	2.98	1.24	0.25	1.00
			A	0.76	1.23	0.37	

TABLE III—*Continued*

M	%Fe[a]	*T* (K)	Site	Δ (mm/s)[b]	δ^{Fe} (mm/s)[c]	Γ (mm/s)[d]	I_B/I_A[e]
	5*	80	B	3.19	1.36	0.32	1.42
			A	2.19	1.30	0.45	
		295	B	2.95	1.24	0.27	1.56
			A	1.41	1.21	0.35	
	1*	80	B	3.16	1.35	0.30	1.46
			A	2.23	1.32	0.32	
		295	B	2.95	1.24	0.24	1.32
			A	1.47	1.21	0.25	
	0.25*	80	B	3.17	1.35	0.27	2.00
			A	2.22	1.32	0.26	
		295	B	2.95	1.24	0.27	1.92
			A	1.47	1.20	0.26	

[a] Compositions labeled with * refer to the use of isotopically enriched ^{57}Fe.
[b] Quadrupole splitting (±0.03 mm/sec).
[c] Isomer shift relative to α-Fe (±0.01 mm/sec).
[d] Full width at half maximum (±0.03 mm/sec).
[e] Intensity ratio of external (B) and internal (A) doublets (±0.20).

nearest-neighbor *M*–O bonding to the site of the Mössbauer probe atom. Although the influence of the neighboring cation on the force constants of the Fe–O bonds are reasonably expected to be negligible, this parameter probably contributes to a small extent to the observed fluctuations.

In the systems Fe–Co, Fe–Ni, and Fe–Mn, the two quadrupole doublets appear with intensities in the ratio between 0.82 and 1.22, corresponding to individual contributions of 50 ± 5%. In the absence of regular or significant variations either with the nature of the associated cation, or with the relative concentration of both elements, Fe^{2+} ions are concluded to be equally distributed between the two available sites.

The situation is quite different in the mixed Fe–Cu system (Fig. 3b) and to a lesser extent in the Fe–Zn compound. As indicated in Table III, highly diluted Fe^{2+} ions occupy preferentially the tetrahydrated site (external doublet, site B) in Cu- and Zn-rich compounds. This observation is fully compatible with the results reported by Ogata *et al.* (*3*) on mixed Cu–Mn, Cu–Ni, and Cu–Zn dihydrated formates. From the nonlinear change in the lattice parameters with the composition of the mixed crystals, they suggested the preferential localization of Cu^{2+} ions in the hexaformato-coordinated A-type site. A more detailed investigation of the equimolar system $Cu_{0.5}Zn_{0.5}(HCO_2)_2 \cdot 2H_2O$ showed that some 70% of the A-type sites were occupied by copper ions (*4*). A similar conclusion was obtained in the frame of EPR measurements on Cu^{2+} ions diluted in a matrix of $Zn(HCO_2)_2 \cdot 2H_2O$ (*25*). Additional confirmations of the definite preference of Cu^{2+} ions for the site surrounded by formate groups exclusively were found in Cu–Mg mixed formates (*5*).

However, we would like to mention the real discrepancy with the Mössbauer results reported some years ago on mixed Fe–Zn, Fe–Mn, Fe–Ni and Fe–Mg systems (*26, 27*). In total disagreement with the present observations, the external doublets of their Mössbauer spectra appear with significantly lower intensities whenever iron is in small concentration (<5%, except for the Fe–Mg system, in which this effect was evidenced from 25% Fe). This peculiar behavior might be the consequence of the particular technique these authors used to obtain their crystals, namely fragmented crystallization from a given parent solution, accompanied by progressive changes in the composition of the mixed crystals as the crystallization proceeded. Our attempts to duplicate these experiments with the Fe–Mn system starting with a 1 : 1 solution from which crystals were collected at regular time intervals over a total period of 1 week were completely unsuccessful ($I_2/I_1 = 0.87 \pm 0.05$ over 8 sampling fractions).

Local configuration of Fe^{2+} ions. Whenever Fe^{2+} ions are incorporated in a formate matrix which is isomorphous with the pure Fe^{2+} compound, the local configuration adopted by these cations in each lattice site is a matter of concern. Independent of possible predominant occupancy of one of the available sites, three different cases can be

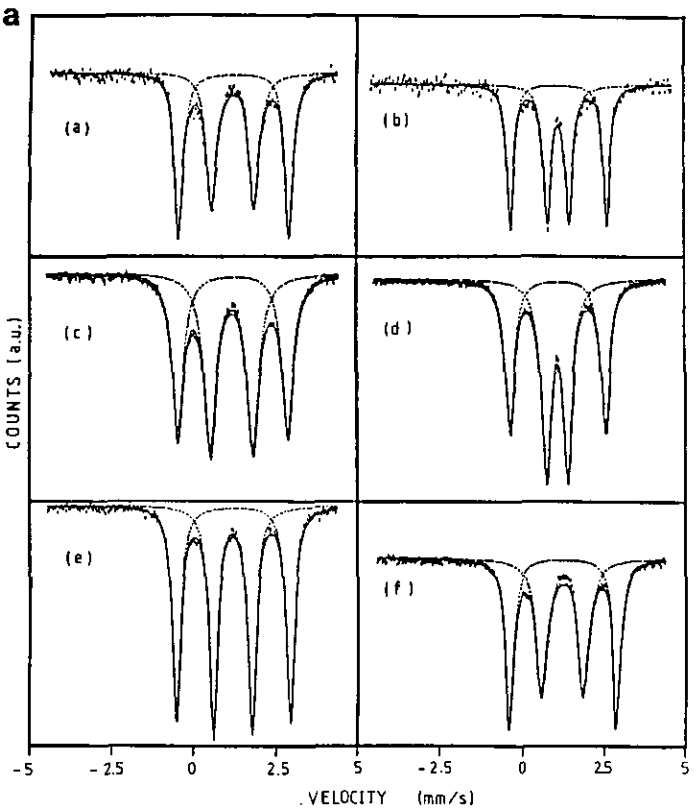

FIG. 3a. ^{57}Fe absorption Mössbauer spectra of $Fe_xM_{1-x}(HCO_2)_2 \cdot 2H_2O$: (a) M = Co, x = 0.50, T = 80 K; (b) M = Co, x = 0.50, T = 295 K; (c) M = Co, x = 0.05, T = 80 K; (d) M = Co, x = 0.05, T = 295 K; (e) M = Mn, x = 0.05, T = 80 K; (f) M = Ni, x = 0.50, T = 80 K.

distinguished. The first possibility consists in finding the Fe^{2+} cations exactly as they would appear in the pure Fe matrix; the second one is the opposite situation, where the iron cations would experience the local symmetry proper to the host cations in their respective sites. The last case to consider is the situation in which the configurational flexibility of the concerned ions allows them to adapt to the local structural strains. The latter option may result in coordination geometries which actually differ from those of the pure iron compound and of the host matrix. Figure 4 illustrates how the RT values of the ^{57}Fe quadrupole splitting associated with the two sites vary with the composition of the mixed compound for different host cations. Figure 5 shows the dependence of the quadrupole splitting at RT and 80 K on the nature of the host cation in the case of the most diluted iron composition (0.5 or 0.25 at.%). The following comments can be made. In the systems Fe–M with M = Mn, Co, Ni, and Zn, the Δ-value is comparable with, although not identical to that of ferrous formate dihydrate and remains fairly unchanged throughout the whole composition range under investigation. When delving a little more into the experimental values, some minor variations can be detected which remain, however, not significant enough to generate coherent and

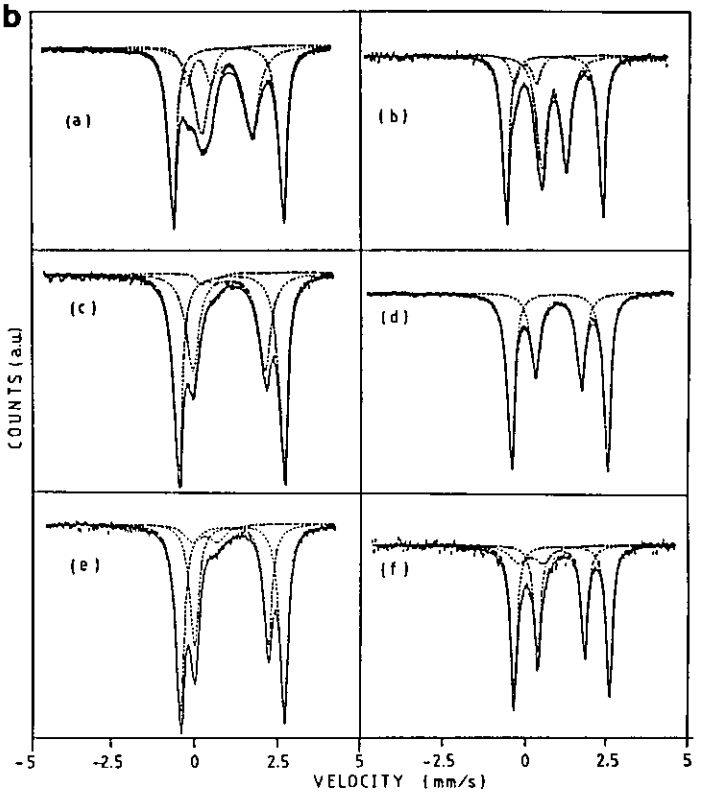

FIG. 3b. ^{57}Fe absorption Mössbauer spectra of $Fe_xCu_{1-x}(HCO_2)_2 \cdot 2H_2O$: (a) $x = 0.50$, $T = 80$ K; (b) $x = 0.50$, $T = 295$ K; (c) $x = 0.05$, $T = 80$ K; (d) $x = 0.05$, $T = 295$ K; (e) $x = 0.01$, $T = 80$ K; (f) $x = 0.01$, $T = 295$ K.

unequivocal interpretations. In line with similar observations mentioned in the dihydrated oxalates (*1*), these changes are most probably due to different contributions of the metal–ligand bonding to the electronic part of the electric field gradient at the nucleus site (see the Appendix). The presence of two different cations on each side of the bridging formate group can be thought responsible for changes in *d–p* overlapping between metal and ligand orbitals. This factor acts on the q_{MO} term as defined in Eq. (9) but the consequences thereof are minimized by the fact that the q_{CF} contribution is definitely predominant for a high-spin ferrous ion.

The mixed iron–copper system behaves differently from the previously described systems. In site A, the Δ-values observed for Fe^{2+} are found to be very sensitive to the composition of the mixed system. In samples with a low iron content, the Δ_A value at RT is about twice that of the corresponding site in pure ferrous formate and is much less sensitive to the temperature. In site B, these peculiarities are clearly less marked. The Δ_B-values are slightly smaller than in the other systems; the lower the temperature, the larger the difference. In addition, whereas no significant dependence of Δ_B on the iron content is noticed at RT, the low temperature values decrease in the Cu-

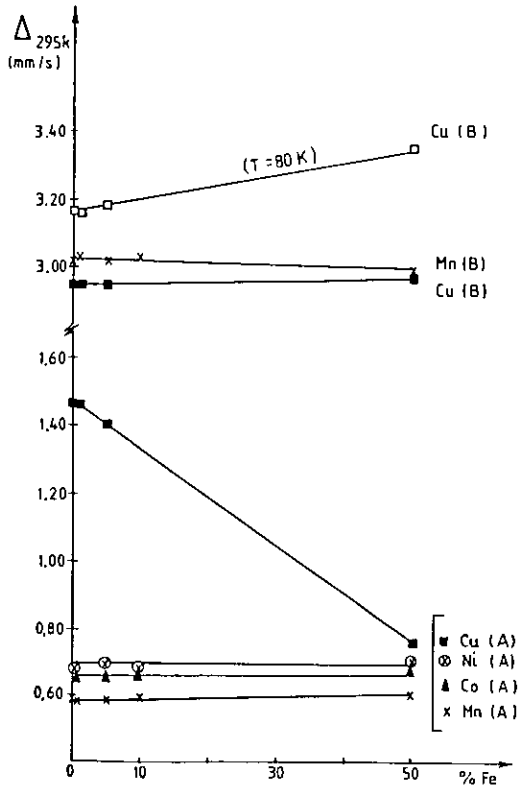

FIG. 4. Quadrupole splitting values of $^{57}Fe^{2+}$ in sites A and B against the composition of the mixed Fe(II)—M(II) dihydrated formates (M = Mn, Co, Ni, Cu).

rich region. To understand this particular behavior, it is necessary to pay close attention to the most relevant characteristics of the crystal structure of copper(II) formate dihydrate. The lattice parameters of $Cu(HCO_2)_2 \cdot 2H_2O$ (Table I) confirm the high tetragonal distortion (z-out type) of the octahedral geometry due to the Jahn–Teller effect, as typical for d^9 ions. A closer look at the structural data of the pure copper compound shows that the elongation axis z of site A is colinear with the Me_1–O_1 direction within the plane containing the formate groups (see Fig. 1). This is not the case for the other formates mentioned in this work, in which the z-axis corresponds to the Me_1–O_4 bond, namely the direction perpendicular to the plane of the sheets. In site B, the elongation axis is oriented toward the Me_2–O_3 direction, i.e., perpendicular to the plane containing the water molecules. As recently confirmed by IR and Raman spectroscopy, the A- and B-type layers are joined to each other by formate bridges in an anti–syn configuration (*28*). The Δ_A-values obtained for Fe^{2+} at 80 K in highly diluted samples are also larger than 2 mm sec^{-1}. This indicates that the Fe^{2+} ions which replace Cu^{2+} in the hexaformato-coordinated site are located in a compressed octahedron, in opposition with the situation observed either in ferrous formate, or in the other bivalent formates considered in this work. Figure 6 schematizes the consequences of

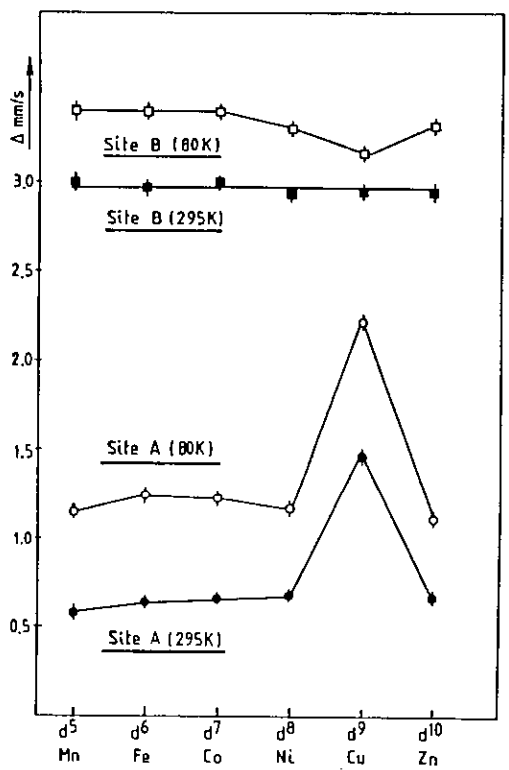

FIG. 5. Quadrupole splitting values of $^{57}Fe^{2+}$ ions at 295 K and 80 K in ^{57}Fe-doped (0.25 or 0.5 at.%) $M(HCO_2)_2 \cdot 2H_2O$.

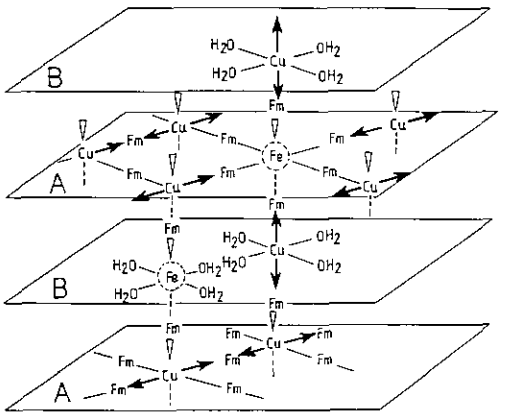

FIG. 6. Schematic representation of the structural configuration of $^{57}Fe^{2+}$ ions diluted in $Cu(HCO_2)_2 \cdot 2H_2O$.

this substitution and can be commented as follows:

(1) In site A, the Fe^{2+} ions are linked through four formate bridging groups to four Cu^{2+} ions lying in the same plane. They are additionally linked along the perpendicular direction, through two other formate groups, to two Cu^{2+} ions of type B, which belong to upper and lower neighboring sheets. The resulting coordination geometry of Fe^{2+} in this site is a compressed octahedron, which corresponds to the elongated one of the Cu^{2+} ions along two different directions, the one within plane A, the other one perpendicular to it.

(2) In site B, substituting Fe^{2+} ions are linked to Cu^{2+} ions only along the axis perpendicular to the plane of the sheets. Because no additional distortion is present along the main axis of the $Fe_B(H_2O)_4(HCO_2)_2$ octahedron, the local geometry adopted by Fe^{2+} ions in this site is essentially equivalent to that in ferrous formate. Consequently, the resulting quadrupole splitting Δ_B is found to be much less sensitive to the substitution effect.

An important conclusion can therefore be drawn about the type of configuration adopted by a host ion or any dopant ion which is incorporated in an isomorphous matrix in the form of mixed crystals. The great sensitivity of the quadrupole splitting values in Mössbauer spectroscopy gives the $^{57}Fe^{2+}$ ions the role of internal probes to characterize the local geometry these ions adopt in a host matrix. The present data related to the Fe–Cu system demonstrate unequivocally that the dopant atom can appreciate the local strains produced by the surroundings and adopts consequently a coordination geometry which is distinct from both that in the pure compound and that of the host cation in its own lattice.

These conclusions fully agree with literature data collected on mixed Cu–Zn formates. First, X-ray diffraction measurements on equimolar mixed crystals $Cu_{0.5}Zn_{0.5}(HCO_2)_2 \cdot 2H_2O$ have evidenced a configuration change in the coordination octahedron of site A, namely that the elongation axis in the mixed compound is preferentially oriented perpendicular to the plane of the sheets, as in the pure zinc compound, and not within this plane, as is the case for the pure copper compound (*4*). Second, EPR investigations on Cu^{2+} ions magnetically diluted in $Zn(HCO_2)_2 \cdot 2H_2O$ have indicated that the copper ions are located in axially elongated octahedra in both crystal sites, the symmetry axis corresponding to the Me_1–Me_2 bond direction, in agreement with the kind of distortion experienced by the pure Zn^{2+} compound (*25*).

The systematic presence of small amounts of Fe^{3+} species in the mixed Fe–Cu compounds (between 5% and 10% of total intensity, up to 25% in the Cu-richest sample) can be understood in a similar way to that previously reported in the case of ^{57}Fe-doped nickel(II) oxalate dihydrate (*1*). The fact that Fe^{2+} ions are easily oxidized when the sample is exposed to ambient air reveals that those ions are most probably located at the surface of the grains. This

location might be the consequence of steric constraints partially preventing the substitutional incorporation of rather large Fe^{2+} ions in strongly compressed lattice sites.

A further comment can be formulated on the mixed equimolar compounds. As shown in Figs. 3a and 3b, the internal doublet in the low-temperature spectra of equimolar Fe–Co, Fe–Ni, and Fe–Cu systems is characterized by a linewidth which is significantly higher than the mean experimental value averaged over all the other compositions. This effect is particularly obvious for the mixed iron–copper compound, with a value of $\Gamma = 0.55$ mm sec^{-1} at 80 K. This line broadening reflects the presence of slightly different quadrupole doublets having the same isomer shift value. They can be assigned to several configurations where the $^{57}Fe^{2+}$ ions in site A are surrounded by one, two, or three nearest-neighboring iron ions in the second coordination sphere. This influence is detected in the hexaformato-coordinated site only, where the central ion is linked to six neighboring cations through the delocalized π-electron system of the bridging formate groups. In the M–M' heterometallic systems for which the structural characteristics of the individual M and M' compounds are similar, such as Fe–Co and Fe–Ni, the occurrence of the former effect is restricted to the low-temperature spectrum, because on lowering the temperature, quadrupole doublets with similar Δ-values become more distinguishable.

Semiquantitative assessment of the t_{2g}-sublevels splitting. As far as the basic assumptions developed in the appendix are accepted (i.e., axial electric field along the z-axis ($\eta = 0$), lattice contribution to the electric field gradient, and spin–orbit coupling neglected) the ratio $\Delta_{80\,K}/\Delta_{300\,K}$ leads to a semi-quantitative assessment of the extent of the tetragonal distortion and allows one to evaluate the importance of metal–ligand interactions. Experimental values of the tetragonal field splitting, Δ_3, and of the covalency parameter, α^2, both calculated from the ratio of the quadrupole splitting values at 295 K and 80 K are presented in Table IV.

TABLE IV

CONFIGURATION OF Fe^{2+} IONS IN $M(HCO_2)_2 \cdot 2H_2O$ (M = Mn, Fe, Co, Ni, Cu, Zn)

M	Mn	Fe	Co	Ni	Cu	Zn
%Fe	0.25	—	0.25	0.5	0.25	0.5
			Site A			
Δ_A (295 K)[a]	0.58	0.64	0.66	0.68	1.47	0.67
Δ_A (80 K)[a]	1.16	1.35	1.33	1.17	2.22	1.11
R_A[b]	2.00	2.11	2.02	1.72	1.51	1.66
G.S.[c]	$\|xz, yz\rangle$	$\|xz, yz\rangle$	$\|xz, yz\rangle$	$\|xz, yz\rangle$	$\|xy\rangle$	$\|xz, yz\rangle$
Δ_3 (cm^{-1})[d]	175	160	170	225	390	240
α^2	0.61	0.75	0.72	0.61	1.56	0.56
			Site B			
Δ_B (295 K)[a]	3.01	2.97	2.95	2.92	2.95	2.95
Δ_B (80 K)[a]	3.40	3.40	3.36	3.30	3.17	3.33
R_B[b]	1.13	1.14	1.14	1.13	1.07	1.13
G.S.[c]	$\|xy\rangle$	$\|xy\rangle$	$\|xy\rangle$	$\|xy\rangle$	$\|xy\rangle$	$\|xy\rangle$
Δ_3 (cm^{-1})[d]	660	645	645	660	785	660
α^2	0.85	0.85	0.85	0.83	0.79	0.83

[a] Δ_A, Δ_B: quadrupole splitting values of doublets A and B.
[b] $R_i = \Delta_i(80\text{ K})/\Delta_i(295\text{ K})$.
[c] G.S. = ground state.
[d] Δ_3: tetragonal field splitting.

Comparing the Δ_3-values obtained for both crystal sites in every host compound but the copper one gives the opportunity to estimate how much larger the tetragonal distortion is in the tetraaquadiformato-coordinated site ($(\Delta_3)_B \approx 650$ cm^{-1}) with respect to the hexaformato-coordinated one ($(\Delta_3)_A \approx 200$ cm^{-1}). The larger axial distortion present in the copper compound is clearly marked for the two crystal sites ($\Delta_A = 390$ cm^{-1}, $\Delta_B = 785$ cm^{-1}), the biggest variation being observed in site A, where the cations are strongly coupled through the formate bridges.

Conclusions

^{57}Fe absorption Mössbauer spectroscopy is shown to be a useful tool to characterize the site occupancy and the local configuration of iron atoms in heterometallic Fe–M

compounds containing structurally non-equivalent lattice sites. In the particular case of the mixed Fe–Cu systems, the coordination geometry of the Fe^{2+} cations in the hexaformato-coordinated sites is found to correspond neither to the situation in the pure iron compound, nor to that one in the pure copper compound. Provided some simplifying assumptions are formulated, the magnitude of the tetragonal distortion around the iron atom can be estimated from the temperature dependence of the ^{57}Fe quadrupole splitting values.

Appendix

The quadrupole splitting Δ is given by the general expression

$$\Delta = \frac{e^2qQ}{2}\left(1 + \frac{\eta^2}{3}\right)^{1/2} = \frac{e^2Q}{2}[(1 - R)q_{val} + (1 - \gamma_\infty)q_{latt}]\left(1 + \frac{\eta^2}{3}\right)^{1/2}, \quad (1)$$

where

e is the elementary charge,

Q is the quadrupole momentum of the Mössbauer probe nucleus,

q_{val} and q_{latt} are the valence and lattice contributions to the electric field gradient (EFG), respectively,

R and γ_∞ are the Sternheimer polarization factors allowing for screening effects, and

η is the asymmetry parameter defined as

$$\eta = \frac{V_{xx} - V_{yy}}{V_{zz}} (0 \le \eta \le 1), \quad (2)$$

where V_{xx}, V_{yy}, V_{zz} are the three main components of the EFG ($|V_{zz}| > |V_{xx}| > |V_{yy}|$).

The temperature dependence of the Δ-value in high-spin ferrous compounds has been described by Ingalls (*29*) and Burbridge *et al.* (*30*). Assuming an electric field with axial symmetry along the z-axis ($V_{xx} = V_{yy} = 0$; $\eta = 0$) and neglecting the spin–orbit coupling, whose contribution remains generally minor, the two partial components of the total EFG can be expressed by

$$q_{val} = \tfrac{4}{7}\langle r^{-3}\rangle_0 \alpha^2 F(\Delta_3, T) \quad (3)$$

and

$$q_{latt} = \pm \frac{14}{3e^2}\frac{\Delta_3}{\langle r^2\rangle}$$

(+ for elongation, − for compression), (4)

where

$\langle r^{-3}\rangle_0$ is a radial factor related to the free ion,

α^2 is the covalency parameter defined according to

$$\langle r^{-3}\rangle_{complex} = \langle r^{-3}\rangle_0 \cdot \alpha^2, \quad (5)$$

Δ_3 is the tetragonal field splitting, and

F is an empirical function describing how the temperature and the tetragonal distortion affect q_{val}.

In the case of tetragonal distortion with $|d_{xy}\rangle$ as ground state (compression),

$$F_{|xy\rangle} = \frac{1 - e^{-\Delta_3/kT}}{1 + 2e^{-\Delta_3/kT}}. \quad (6)$$

For an elongation ($|d_{xz}, d_{yz}\rangle$ as ground state),

$$F_{|xz,yz\rangle} = -\frac{1 - e^{-\Delta_3/kT}}{2 + e^{-\Delta_3/kT}}. \quad (7)$$

As the temperature is lowered ($T \to 0$ K), $F_{|xy\rangle}$ and $F_{|xz,yz\rangle}$ approach $+1$ and -0.5, respectively. If the lattice contribution to the EFG is further neglected, the two situations result in quadrupole splittings of opposite sign whose maximum values are in the ratio 2 : 1.

The valence contribution can be developed according to

$$q_{val} = \tfrac{4}{7}\langle r^{-3}\rangle_{3d}[-n_{3d_{z^2}} + n_{3d_{x^2-y^2}} + n_{3d_{xy}} - \tfrac{1}{2}(n_{3d_{xz}} + n_{3d_{yz}})],$$

where the n_{3d_i} terms represent the respective $3d$-orbital population, and can be further separated into two major components corresponding to the crystal field (q_{CF}) and molecular orbitals (q_{MO}) contributions (*31*), namely

$$q_{val} = q_{CF} + q_{MO}. \qquad (9)$$

q_{CF} represents the contributions of valence electrons in the purely electrostatic crystal field model; q_{MO} allows for metal–ligand orbital overlapping and describes the covalency effects via σ- or π-electron density transfer. For high-spin ferrous ions, q_{CF} is definitely predominant.

The covalency parameter α^2 defined in Eq. (5) characterizes the radial expansion of t_{2g} orbitals in direct relation with the nephelauxetic parameter. This parameter usually takes values between 0.6 and 0.9; the lower α^2, the larger the covalency effects. An empirical estimation of this parameter can be carried out using the Ingalls–Burbridge model with the following restrictions: axial distortion ($\eta = 0$; $\Delta_1 = \Delta_2 = \Delta_3$), spin–orbit coupling, and q_{latt} neglected. Assuming a given type of axial distortion, compression, or elongation in relation to the experimental data of the crystal structure when available, Δ_3 can be calculated from the ratio $\Delta_{80K}/\Delta_{300K}$. Hence, the α^2-parameter can be obtained from the ratio between the experimental Δ-value at a given temperature and the theoretical limiting value corresponding to $\alpha^2 = 1$, according to

$$\frac{\Delta(T)}{\Delta_{max}} = \frac{\alpha^2 \cdot F(\Delta_3, T)}{F_{max}}, \qquad (10)$$

where Δ_{max} and F_{max} are taken respectively as $+4$ mm.s^{-1} and $+1$ for an axially compressed octahedron and as -2 mm.s^{-1} and -0.5 for an axially elongated octahedron.

Acknowledgment

The authors gratefully acknowledge the "Institut Interuniversitaire des Sciences Nucléaires," Brussels, for financial support.

References

1. M. Devillers, J. Ladrière, and D. Apers, *Inorg. Chim. Acta* **126,** 71 (1987).
2. M. Devillers, J. Ladrière, and D. Apers, *J. Phys. Chem. Solids* **49,** 909 (1988).
3. T. Ogata, T. Taga, and K. Osaki, *Bull. Chem. Soc. Jpn.* **50**(7), 1674 (1977).
4. T. Ogata, T. Taga, and K. Osaki, *Bull. Chem. Soc. Jpn.* **50**(7), 1680 (1977).
5. D. Stoilova, C. Balarew, and V. Vassileva, *Izv. Otd. Khim. Nauki (Bulg. Akad. Nauk.)* **18,** 3 (1985).
6. D. Stoilova and S. Angelov, *J. Solid State Chem.* **82,** 60 (1989).
7. D. Stoilova and A. Aslanian, *Process. Technol. Proc.* **6** (*Ind. Cryst.*, 1987), 271 (1989).
8. G. Weber, *Acta Crystallogr. Sect. B* **36,** 3107 (1980).
9. M. I. Kay, I. Almodovar, and S. F. Kaplan, *Acta Crystallogr. Sect. B* **24,** 1312 (1968).
10. A. S. Antsyshkina, M. K. Guseinova, and M. A. Porai-Koshits, *J. Struct. Chem.* **8,** 321 (1967) [*Zh. Strukt. Khim.* **8**(2), 365 (1967)].
11. K. Krogmann and R. Matters, *Z. Kristallogr.* **118,** 291 (1963).
12. M. Bukowska-Strzyzewska, *Acta Crystallogr.* **19,** 357 (1965).
13. N. Burger and H. Fuess, *Z. Kristallogr.* **145,** 346 (1977).
14. G. De With, S. Harkema, and G. J. Van Hummel, *Acta Crystallogr. Sect. B* **32,** 1980 (1976).
15. M. L. Post and J. Trotter, *Acta Crystallogr. Sect. B* **30,** 1880 (1974).
16. M. Matsuura, K. Takeda, T. Satoh, Y. Sawada, and J. M. Machado Da Silva, *Solid State Commun.* **13,** 467 (1973).
17. P. Burlet, J. Rossat-Mignod, and M. Matsura, *J. Phys. Lett.* **40,** L-455 (1979).
18. P. Burlet, P. Burlet, J. Rossat-Mignod, A. De Combarieu, and E. Bedin, *Phys. Status Solidi b* **71,** 675 (1975).
19. G. R. Hoy, S. de S. Barros, F. de S. Barros, and S. A. Friedberg, *J. Appl. Phys.* **36**(3), 936 (1965).
20. M. Inoue and M. Kubo, *Inorg. Chem.* **9**(10), 2310 (1970).
21. J. Ladrière and D. Apers, *J. Phys. Colloq.* **C6**(37), C6-913 (1976).
22. G. R. Hoy and F. de S. Barros, *Phys. Rev.* **139**(3A), 929 (1965).
23. K. Muraishi, T. Takano, K. Nagase, and N.

TANAKA, *J. Inorg. Nucl. Chem.* **43**(10), 2293 (1981).
24. J. LADRIÈRE AND D. APERS, *in* "Abstracts of the International Conference on the Applications of the Mössbauer Effect, Alma-Ata, USSR, p. 147 (1983).
25. G. R. WAGNER, R. T. SCHUMACHER, AND S. A. FRIEDBERG, *Phys. Rev.* **150**(1), 226 (1966).
26. K. NAGORNY AND J. F. MARCH, *Z. Phys. Chem.* **78,** 311 (1972).
27. J. F. MARCH, G. WEBER, AND K.NAGORNY, *Z. Phys. Chem.* **85,** 97 (1973).
28. R. O. CARTER, III, B. D. POINDEXTER, AND W. H. WEBER, *Vibr. Spectrosc.* **2,** 125 (1991).
29. R. INGALLS, *Phys. Rev.* **133**(3A), 787 (1964).
30. C. D. BURBRIDGE, D. M. L. GOODGAME AND M. GOODGAME, *J. Chem. Soc.* (A), 349 (1967).
31. G. M. BANCROFT, "Mössbauer Spectroscopy," McGraw–Hill, London (1973).